Since January 2020 Elsevier has created a COVID-19 resource centre with free information in English and Mandarin on the novel coronavirus COVID-19. The COVID-19 resource centre is hosted on Elsevier Connect, the company's public news and information website.

Analytica Chimica Acta 1230 (2022) 340389

Contents lists available at ScienceDirect

Analytica Chimica Acta

journal homepage: www.elsevier.com/locate/aca

Fluorescent nanodiamond-based spin-enhanced lateral flow immunoassay for detection of SARS-CoV-2 nucleocapsid protein and spike protein from different variants

Wesley Wei-Wen Hsiao [a,*,1], Neha Sharma [a,1], Trong-Nghia Le [b], Yu-Yuan Cheng [a], Cheng-Chung Lee [c,d], Duc-Thang Vo [e], Yuen Yung Hui [b], Huan-Cheng Chang [a,b], Wei-Hung Chiang [a,**]

[a] Department of Chemical Engineering, National Taiwan University of Science and Technology, Taipei, Taiwan
[b] Institute of Atomic and Molecular Sciences, Academia Sinica, Taipei, Taiwan
[c] Institute of Biological Chemistry, Academia Sinica, Taipei, Taiwan
[d] The Ph.D. Program for Translational Medicine, College of Medical Science and Technology, Taipei Medical University, Taipei, Taiwan
[e] College of Engineering, National Taiwan University of Science and Technology, Taipei, Taiwan

HIGHLIGHTS

- Sensitive detection of SARS-CoV-2 N and S antigens from wild-type, Alpha, Delta, and Omicron variants in artificial saliva.
- Our direct SELFIA assay can be used for antibody/antigen pair screening.
- Our competitive SELFIA assay serves as a precise quantitative diagnostic tool.

GRAPHICAL ABSTRACT

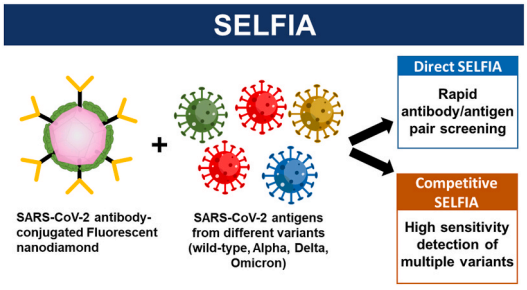

ARTICLE INFO

Keywords:
COVID-19 pandemic
SARS-CoV-2
SELFIA
Fluorescent nanodiamond

ABSTRACT

SARS-CoV-2 viruses, responsible for the COVID-19 pandemic, continues to evolve into new mutations, which poses a significant threat to public health. Current testing methods have some limitations, such as long turn-around times, high costs, and professional laboratory requirements. In this report, the novel Spin-Enhanced Lateral Flow Immunoassay (SELFIA) platform and fluorescent nanodiamond (FND) reporter were utilized for the rapid detection of SARS-CoV-2 nucleocapsid and spike antigens from different variants, including wild-type (Wuhan-1), Alpha (B.1.1.7), Delta (B.1.617.2), and Omicron (B.1.1.529). The SARS-CoV-2 antibodies were conjugated with FND via nonspecific binding, enabling the detection of SARS-CoV-2 antigens via both direct and competitive SELFIA format. Direct SELFIA was performed by directly adding the SARS-CoV-2 antibodies-conjugated FND on the antigens-immobilized nitrocellulose (NC) membrane. Conversely, the SARS-CoV-2 antigen-containing sample was first incubated with the antibodies-conjugated FND, and then dropped on the antigen-

* Corresponding author.
** Corresponding author.
E-mail addresses: weshsiao@mail.ntust.edu.tw (W. Wei-Wen Hsiao), whchiang@mail.ntust.edu.tw (W.-H. Chiang).
[1] These authors contributed equally to this work.

https://doi.org/10.1016/j.aca.2022.340389
Received 3 May 2022; Received in revised form 30 August 2022; Accepted 9 September 2022
Available online 14 September 2022

immobilized NC membrane to carry out the competitive SELFIA. The results suggested that S44F anti-S IgG antibody can be efficiently used for the detection of wild-type, Alpha, Delta, and Omicron variants spike antigens. Findings were comparable in direct SELFIA, competitive SELFIA, and ELISA. A detection limit of 1.94, 0.77, 1.14, 1.91, and 1.68 ng/mL can be achieved for SARS-CoV-2 N protein, wild-type, Alpha, Delta, and Omicron S proteins, respectively, via competitive SELFIA assay. These results suggest that a direct SELFIA assay can be used for antibody/antigen pair screening in diagnosis development, while the competitive SELFIA assay can serve as an accurate quantitative diagnostic tool. The simplicity and rapidity of the SELFIA platform were demonstrated, which can be leveraged in the detection of other infectious diseases in the near future.

1. Introduction

The global spread of SARS-CoV-2 prompted the World Health Organization (WHO) to declare COVID-19 a pandemic on March 12, 2020 [1,2]. Many countries have been doing social distancing and lockdowns due to the disease's rapid transmission. According to the WHO, as of March 2022, SARS-CoV-2 has infected 480 million people and caused more than 6 million deaths. The wild-type (Wuhan-1) continues to evolve into different mutations, such as B.1.1.7 (Alpha), B1.351 (Beta), P.1 (Gamma), B.1.617.2 (Delta), and B.1.1.529 (Omicron) [3–5]. Mostly, a new variant is more contagious than the wild type [6]. Thus, some of its effects may change, such as how fast the virus spreads and the effect of vaccinations on new mutations. For example, for the Delta variant, viral infections occurred at similar rates in unvaccinated and vaccinated persons, although the duration of viral infection may have been reduced in vaccinated persons [5].

Testing, tracking infected people, and contact tracing are important tools for reducing the pandemic's spread. A diagnostic test should have sufficient sensitivity and accuracy to ensure rapid treatment decisions [7]. Several testing methods have been studied and used for SARS-CoV-2 diagnoses, such as nucleic acid amplification tests (Reverse transcription-polymerase chain reaction, RT-PCR, and the clustered regularly interspaced short palindromic repeats, CRISPR), the serology-based tests (enzyme-linked immunosorbent assay (ELISA), lateral flow immunoassay (LFIA), or other tests (CT scan, Biosensor) [7–10]. Analytical efficiency, affordability, and ease of use should be considered in evaluating the application's ability. The most reliable and accurate test for COVID-19 is RT-PCR, Reverse transcription loop-mediated isothermal amplification (RT-LAMP), Reverse transcription-quantitative polymerase chain reaction (RT-qPCR), and CRISPR [7,10]. However, these methods are not ideal screening procedures for mass screening since they are expensive, time-consuming (~24 h), and require well-equipped laboratories and trained professionals [11].

In serological tests, COVID-19 infection can be detected directly through viral RNA or indirectly with the serum's host-specific antibodies (IgG, IgA, IgM) [7]. Several studies used antibodies to detect viruses directly, but the affinity of most antibodies is not sufficient to detect small numbers of virus particles [7]. In addition, interferents (interferon, rheumatoid factor, and non-specific IgM) and low sensitivity have caused problems in immunoassays [7]. IgG and IgM are expressed at least three days after infection which limits the detection of those antibodies since they can produce false-negative results during the disease's early stages [7,11].

On the other hand, the detection of viral antigens can ensure rapid detection. The SARS-CoV-2 virus consists of four structural proteins: the N protein (nucleocapsid) holds the RNA genome, the S (spike), M (membrane), and E (envelop) proteins create the envelope [2,7,12,13]. The S and N proteins are highly immunogenic proteins during infection and are frequently used in serological assays [7,12–15]. S protein is the major surface protein antigen of SARS-CoV-2 and is considered the best-suited antigen for the direct detection of SARS-CoV-2 due to its high antigenicity and specificity compared to other coronaviruses [16]. However, observed mutations in SARS-CoV-2, which exhibit changes in the viral nucleic acid and protein sequences, jeopardizes the utility of certain *in vitro* diagnostic assays [13,17,18]. Mostly, the S protein undergoes a mutation leading to false-negative results because of weak binding affinity between the mutants and existing antibodies [13,17]. It is therefore required to qualify more than one antibody isotype-viral protein interaction with high sensitivity. Xi et al. indicated that developing reliable and efficient biosensors are urgent for the detection and analysis of SARS-CoV-2 variants [13]. Agarwal et al. demonstrated that the microcantilever-based test for SARS-CoV-2 could identify wild-type and Alpha variants at a clinically relevant concentration down to 1 ng/mL [19]. Lee et al. found that ACE2-based biosensors were able to detect S antigens from wild-type, Alpha, and Beta variants with a detection limit of 10 ng/mL, 0.5 ng/mL, and 10 ng/mL, respectively [20]. However, there has been a lack of research on the ability of these methods to identify other COVID variants, such as the currently more contagious Delta and Omicron variants.

Recently, many antigen-targeted LFIA tests have been developed and marketed to alleviate the pandemic's diagnostic burden [11]. Although they are faster, less expensive, and simpler than RT-PCR, these LFIA tests are limited in sensitivity and accuracy. Sample enrichment, signal amplification, and assay optimization have all been mobilized to help overcome this problem. For example, the RT-LAMP-based LFIA assay of SARS-CoV-2 can detect the viral RNA in 40 min at a detection limit of 2 copies/μL [21]. However, limitations for these amplification LFIA systems remain, such as costly reagents and equipment, and multiple steps. Among those methods, the use of fluorescent nanoparticles with fluorescent readout seems more promising for achieving accurate quantitative and qualitative tests. Fluorescent nanodiamond (FND), with a high density of negatively charged nitrogen-vacancy (NV^-) centers, has been considered an excellent alternative reporter for LFIA due to the fact that it is highly stable, non-photobleaching, non-photoblinking, highly biocompatible, and amenable to surface modification [11,22]. In addition, FND exhibit a longer lifetime, higher quantum yield, and infinite photostability compared with organic dyes. As a result, FND is considered as a highly efficient fluorescent probe [23]. Researchers found that FNDs with surface functionalization with carboxylic group (-COOH) have higher absorption properties [24]. Different functional groups on the surface of FNDs are able to bind with biological molecules such as proteins, enzymes, virus antigens, antibodies, and nucleic acids [25].

In this work, we developed FND-based Spin Enhanced Lateral Flow Immunoassay (SELFIA) to detect SARS-CoV-2 nucleocapsid and spike antigens. Spike proteins from different SARS-CoV-2 variants, including wild-type, Alpha, Delta, and Omicron, were used to investigate the antibody/antigen binding affinity. The S44F anti-S IgG antibody exhibited binding affinity to all three SARS-CoV-2 variants through direct immunoassays. The competitive SELFIA assay was performed by mixing antibodies-conjugated FND and known concentrations of SARS-CoV-2 antigens. Results indicated that the direct SELFIA assay might be used to evaluate antibody/antigen pairs in the development of early diagnostics, while the competitive SELFIA assay could be utilized as an accurate quantitative diagnosis tool, as it exhibited enhanced sensitivity of SARS-CoV-2 N and S antigens detection compared to direct assays.

2. Materials and methods

2.1. Materials

FNDs (diameter ~100 nm) were produced using high-energy ion radiation of synthetic diamond powder (micro + MDA M0.10), followed by air oxidation (450 °C), vacuum annealing (800 °C), and acidic wash in H_2SO_4–HNO_3 (at 100 °C) [26,27]. Bovine serum albumin (BSA) was obtained from Sigma Aldrich. Spike protein of SARS-CoV-2 from different variants (Wild-type, Alpha-type, Delta-type, Omicron-type), SARS-CoV-2 nucleocapsid protein (Wild-type), and SARS-CoV-2 anti--spike IgG antibody (S44F), anti-chicken SARS-CoV-2 IgG-S8 nucleocapsid protein antibody were purchased from Pharmtekx Co. Ltd. Phosphate-buffered saline (PBS) solution and artificial saliva were prepared in the laboratory. All reagents were used directly without any further purification.

2.2. FND-antibody conjugates

SARS-CoV-2 S44F and S8-IgG antibodies were conjugated with FND through nonspecific binding, as described in Fig. S1. Briefly, FND containing solution (1 mg/mL) was first sonicated for 5–10 s. Then, the antibody solution was mixed with FND at a ratio of 1:5 (w/w) at room temperature for 20 min. The BSA (3%) in DI water solution was added and the mixture was then centrifuged for 5 min at 20000 g to remove the unbound protein. The BSA in PBS (BSA/PBS, 3%) was added to obtain the stock solution of antibody-conjugated FND at a concentration of 100 ng/μL. The stock solution was stored at 4 °C until use.

2.3. Direct SELFIA assay

To perform the immunoassays, SARS-CoV-2 antigens (1 μL) at different concentrations were first deposited at the centers of the nitrocellulose (NC) membrane (Millipore, FF120HP plus) and allowed to dry at room temperature. The test strip was pre-wetted with 30 μL of 3% BSA/PBS solution for 5 min. Subsequently, 100 μL of the antibody-conjugated FND solution (1 ng/μL) was suspended on the sample pad. The strip was then placed at room temperature for 30 min and dried at 50 °C for 2 min prior to the SELFIA measurement. Artificial saliva and BSA/PBS solution (3%) were used to dilute the antigen and the antibody-conjugated FND stock solution, respectively.

2.4. Competitive assay

SARS-CoV-2 antigens were first prepared at different concentrations in 3% BSA/PBS, including 1 μg/mL, 100 ng/mL, 10 ng/mL, 5 ng/mL, 1 ng/mL, 0.1 ng/mL, 0 ng/mL. After that, 10 μL of the antibody-conjugated FND solution (10 ng/μL) was incubated with 100 μL of the antigen solution for 30 min at room temperature. 30 μL of 3% BSA solution in PBS was added to test strips with immobilized SARS-CoV-2 antigen (1 μg) at the centers of the NC membrane and left for 5 min. Subsequently, 100 μL of the antigen-binding antibody-conjugated FND mixture solution was suspended on the strip. The strip was then placed at room temperature for 30 min and dried at 50 °C for 2 min prior to the SELFIA measurement.

2.5. SELFIA measurement

The SELFIA system was described in our previous report to quantify the FND captured on the NC membrane of the LFIA strip [28]. The major component of the system was composed of a lock-in amplifier to drive an electromagnetic coil and produce an Alternative Current (AC) magnetic field. The resultant AC magnetic field was operated at the frequency of 102.4 Hz with the field strength of B = 40 mT. The fluorescence signal from the LFIA strip was modulated by the AC magnetic field and then analyzed with the lock-in amplifier of SELFIA. Since only the FND fluorescence signal can be modulated by the magnetic field, SELFIA extracted the FND signal from the NC membrane background and enhanced the detection limit for FND in the LFIA strip.

3. Result and discussion

3.1. SARS-CoV-2 antibodies-conjugated FND

The photoluminescence (PL) spectra of pure FND in deionized water (1 mg/mL) are shown in Fig. 1a. The FND was excited at 530–560 nm and exhibited fluorescence signals at ~700 nm without the photo-blinking and photo-bleaching effects. Hence, a green laser (532 nm) was used as an incident light on the sample strip to detect the SARS-CoV-2 antibodies conjugated FNDs captured by antigens in SELFIA. The size and morphology of FND were observed by UHR-CFE-SEM TE-Driver (Hitachi High-Technologies and Bruker Corporation) and shown in Fig. 1b. The average size is about 100 nm.

3.2. Direct SELFIA assay

Direct LIFA is a regularly used test format during the early stages of assay development for a "full" LFIA [29]. The strip is composed of a NC membrane and an absorbent pad. Both the NC membrane and the absorbent pad are 4 mm wide and are bound together on a low fluorescence backing card. 1 μL of the antigen of interest with known concentration was immobilized on the center of the NC membrane and dried at room temperature. To carry out the assay, the NC membrane binding site was first blocked by pre-wetting with 30 μL of 3% BSA solution in PBS for 5 min. Subsequently, 100 ng of antibodies-conjugated FND (100 μL) was added into the test cassette sample well. The test liquids can be driven through the porous network of the NC membrane by capillary force and are eventually absorbed by the absorbent pad. The test strip was then dried, and the fluorescent intensity was measured by the SELFIA platform.

The SELFIA platform provides a continuous laser and lock-in detection method through magnetic modulation with a photomultiplier tube as a detector. In this system, a continuous-wave green laser (532 nm, 10 mW) excited the FND present on the NC membrane of the LFIA strip in the presence of a magnetic field ($f = 102.4$ Hz, $B = 40$ mT). The resulting FND signal was collected using an objective lens, long-pass filter and detected by a photomultiplier tube [28]. Fig. 2 shows the fluorescent spectra of the FND captured by the SARS-CoV-2 antigens on the strip. The anti-chicken anti-N IgG (S8) antibody was used to detect the SARS-CoV-2 N protein. A distinct peak of FND mass can be observed when the N protein concentration is at 100 μg/mL (Fig. 2b). The dose-response curves of the fluorescent integrated intensity of FND captured on the strip by SARS-CoV-2 N protein concentrations are shown in Fig. 2c. The experimental data fit with a logistic function.

Similarly, the FND mass intensity could also be observed for the detection of SARS-CoV-2 S protein from different variants using the S44F anti-S antibody-conjugated FND (Fig. 3a–d). It is noted that the S44F antibody could efficiently bind with either wild-type, Alpha, Delta, or Omicron variants S antigens. The dose-response curves of the fluorescent integrated intensity of FND captured on the strip by different antigen concentrations are shown in Fig. 3e. The experimental data fit with a logistic function. It was observed that the fluorescent intensity is saturated at a high concentration of the antigen (~1000 μg/mL). According to the integrated fluorescence intensity of the whole 4 mm bands, the binding effectiveness between S44F antibody-conjugated FND and wild-type or Delta variant proteins on the strip was approximately 100%. In addition, the results suggest that S44F antibodies have a greater binding affinity to wild-type and Delta variants' S antigens compared with Alpha S antigen. We then compared the binding ability of the S44F antibody in direct SELFIA with ELISA. The direct ELISA protocol is described in Supporting Information, and the results are shown in Fig. S2. It was found that S44F antibody could be efficiently

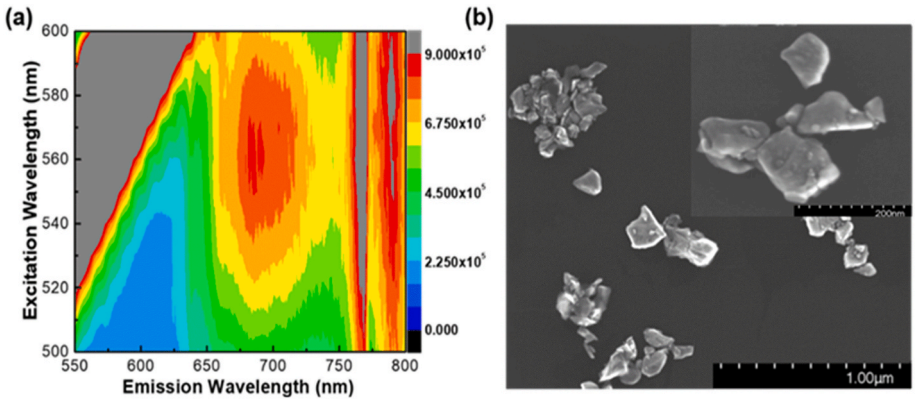

Fig. 1. (a) Photoluminescence spectra of pure FND in deionized water (1 mg/mL), and (b) Dark field UHRSTEM of FND.

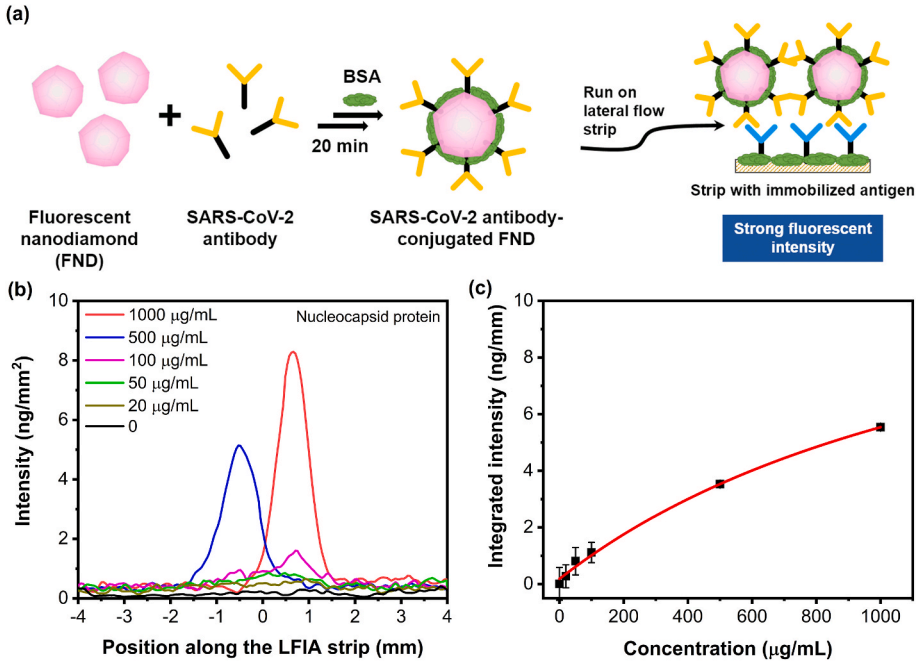

Fig. 2. Illustration of direct SELFIA assays with FND reporter (a). In direct SELFIA, antigens were dropped on the NC membrane and Ab-conjugated FND solution was dropped on sample pad. As the solution flowed towards the absorption pad, Ab-conjugated FND was captured by the antigen dropped on the NC membrane, generating a fluorescent signal when measured with the SELFIA platform. FND fluorescent spectra (b) and calibration curve (c) via direct SELFIA assays in artificial saliva for SARS-CoV-2 nucleocapsid antigen using anti-chicken IgG antibody-conjugated FND (b). The solid curve is the best fit of the experimental data to a logistic function, $y = a_2 + (a_1 + a_2)/(1 + (x/x_0)^p)$, where a_1, a_2, x_0, and p are constants. (n = 3).

captured by wild-type, Alpha, and Delta variants' S proteins, while only a small amount of S44F antibody could be captured by Omicron S protein in ELISA. The difference in Omicron S protein detection between direct SELFIA and ELISA can be explained due to the non-specific binding in SELFIA assay or the insufficient capturing of antibodies in ELISA. To prove no nonspecific binding with other proteins, we subsequently conducted direct SELFIA using FND-S44F with immobilized N protein on the strip. As shown in Fig. S3, no FND signal could be observed at a very high concentration of N protein (1000 ng/mL), providing solid evidence for eliminating the doubt of non-specific binding in direct SELFIA. According to previous studies [30,31], due to inadequate blocking of the surface of the microplate coated with antigen, the ELISA might sometimes report false-negative results. Competitive assay using SELFIA had a very low detection limit, demonstrating that the technique can provide accurate results, even with low sample concentrations. We used LFIA strips for the SELFIA method. LFIA strips are the gold standard. In SELFIA, we use fluorescence nanodiamond. To get a fluorescence signal a SELFIA device must be used. Using SELFIA can also reduce false-negative results, as it is able to emit a highly-sensitive signal even at very low sample concentrations.

The detection limits (LOD) by direct SELFIA assay for SARS-CoV-2 N and S proteins are shown in Table 1. The LOD values of SARS-CoV-2 N protein, wild-type, Alpha, Delta, and Omicron S proteins in artificial saliva were 1.5, 0.05, 0.53, 0.04, and 0.09 μg/mL, respectively, determined as the mean of blank + 3SD. Although the detection of wild-type, Delta, and Omicron S proteins is the most sensitive, 40–90 ng/mL (0.20–0.45 nM), among the tested antigens via direct SELFIA, the LOD is relatively high compared to other LFIA assays coupled with a signal readout. This is because we used only 1 μL of the sample in our assay, which suggests that the SELFIA platform can detect up to 40–90 pg of the S antigen. The rapid and simple nature of the direct SELFIA assay indicates that it can be utilized for antibody/antigen screening. The SELFIA platform can efficiently determine an antibody/antigen pair with high binding affinity, which is crucial for accurate diagnosis, especially in the event of a new infectious disease outbreak. Further development of the competitive SELFIA assay was carried out to enhance sensitivity since larger samples can be used in this format.

3.3. *Competitive immunoassay SARS-CoV-2*

To perform the competitive assay, the antibody-conjugated FND was incubated with the sample for 30 min, and the mixture was dropped on the test strip. For samples that contained the analyst antigens, the antigens bound with the antibody-conjugated FND at the incubation step,

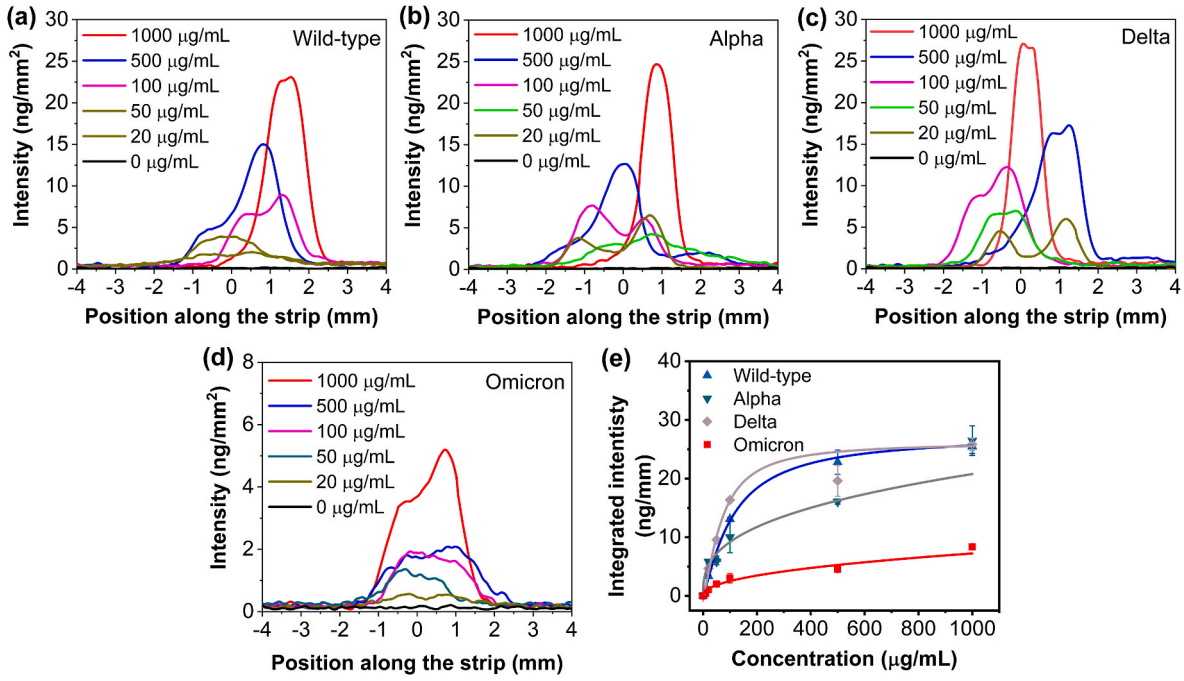

Fig. 3. FND fluorescent spectra via direct SELFIA assays in artificial saliva SARS-CoV-2 spike antigen from (a) wild-type, (b) Alpha, (c) Delta, and (d) Omicron variants using S44F antibody-conjugated FND. (e) Calibration curve for the detection of SARS-CoV-2 S antigens in artificial saliva. The solid curve is the best fit of the experimental data to a logistic function, $y = a_2 + (a_1 + a_2)/(1 + (x/x_0)^p)$, where a_1, a_2, x_0, and p are constants. (n = 3).

Table 1
Detection limit of direct and competitive SELFIA assay for SARS-CoV-2 antigens.

Analyst	Direct SELFIA (μg mL^{-1})	Competitive assay (ng mL^{-1})
SARS-CoV-2 Nucleocapsid protein	1.50	1.94
SARS-CoV-2 Wild-type Spike protein	0.05	0.77
SARS-CoV-2 Alpha Spike protein	0.53	1.14
SARS-CoV-2 Delta Spike protein	0.04	1.91
SARS-CoV-2 Omicron Spike protein	0.09	1.68

and therefore, the Ab-conjugated FND was not captured by the antigen immobilized on the strip (Fig. 4a). No signal or less signal intensity can be observed compared to the blank. For samples that did not contain the analyst antigens or blank sample, the antibody-conjugated FND was captured by the antigen immobilized on the strip and therefore generated high signal intensity. Fig. 4b–c shows the competitive SELFIA results for SARS-CoV-2 N antigen detection. Without N antigen (0 ng/mL), a distinct and strong fluorescent peak of FND was observed along the strip (Fig. 4b). The peak decreased with increasing N antigen concentrations and disappeared at 1000 ng/mL of N antigen in the sample. The normalized intensity is shown in Fig. 4c. The LOD was determined to be 1.94 ng/mL for SARS-CoV-2 N antigen detection.

The competitive SELFIA assays for SARS-CoV-2 S antigen detection were investigated and are shown in Fig. 5. Similar to N antigen detection, without the presence of the antigen of interest, the S44F antibody-conjugated FND was captured on the strip and exhibited a strong fluorescent signal. The FND fluorescent peaks for SARS-CoV-2 wild-type, Alpha, Delta, and Omicron S antigens are shown in Fig. 5a–d. To compare the detection of SARS-CoV-2 S antigens from different variants, the normalized integrated fluorescent intensity was obtained and is shown in Fig. 5e. The LOD via competitive SELFIA was calculated and is shown in Table 1. It was found that the LOD values of SARS-CoV-2 wild-type, Alpha, Delta, and Omicron S proteins were 0.77, 1.14, 1.91, and 1.68 ng/mL, respectively. Compared to the direct format, the sensitivity of competitive SELFIA was improved 50-fold, which can be attributed to the use of a larger sample size.

SARS-CoV-2 detection by the SELFIA platform was demonstrated in both direct and competitive formats. Another format, sandwich assay, is also frequently used for rapid tests. Many sandwich SARS-CoV-2 tests have been developed and commercialized [11]. Our work focused on the SARS-CoV-2 antibody (S44F) that enables the detection of SARS-CoV-2 variants. This is more crucial since the SARS-CoV-2 virus is continually mutating and affecting diagnosis and treatment outcomes. The finding of another antibody that can capture many SARS-CoV-2 spike variants at a different epitope to S44F poses a challenge to the development of sandwich assays. Perhaps the S44F antibody can be used as a capture antibody in combination with commercially available antibodies for specific SARS-CoV-2 variants to enable variant identification. This is more promising for variant identification and disease surveillance since the SELFIA platform can provide rapid results compared with the costly and time-consuming assays of frequently used nucleic acid amplification tests (NAATs). Our competitive SELFIA was demonstrated to be very sensitive, with a LOD of approximately 4.4–11.0 pM for the SARS-CoV-2 spike from different variants. A comparison of LOD between this report and other studies is presented in Table S1. Apart from that, the competitive format was reported to provide a wider detection range and can be effective at the range that the Hook effect occurred [32].

In a recent study, the nitrogen-vacancy (NV) centers in nanodiamonds (NDs) were used for SARS-CoV-2 RNA detection [33]. The NDs were first noncovalently coated with polyethyleneimine (PEI), a polymer capable of forming reversible complexes with viral complementary DNA sequences, and incorporated with magnetic molecules (gadolinium, Gd^{3+}) to form the c-DNA-DOTA-Gd^{3+} hybrid. In a positive sample, the viral RNA forms a complex with the c-DNA-DOTA-Gd^{3+} and diffuses through the solution, increasing the distance between Gd and ND. The magnetic noise induced by Gd is reduced, leading to a longer relaxation time of the NV center. The method was reported to achieve high sensitivity of a few hundreds of RNA copies with less than a 1% false-negative fate. However, the preparation of the hybrid is

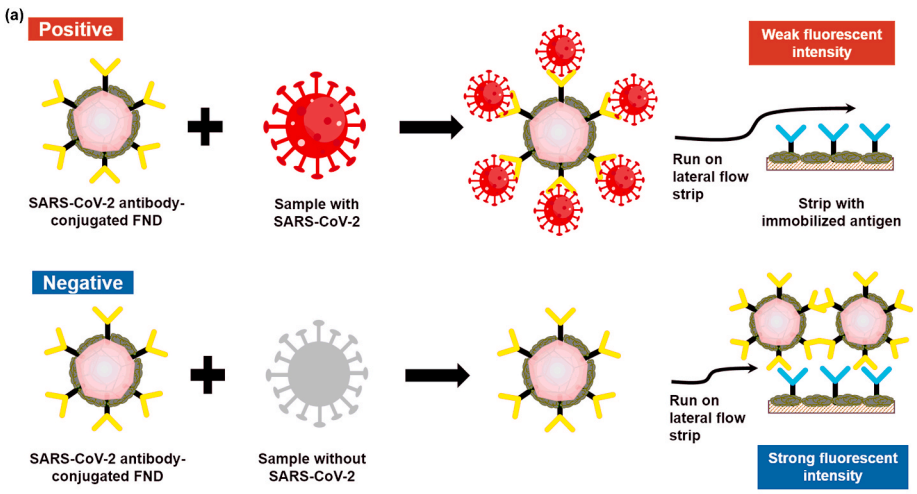

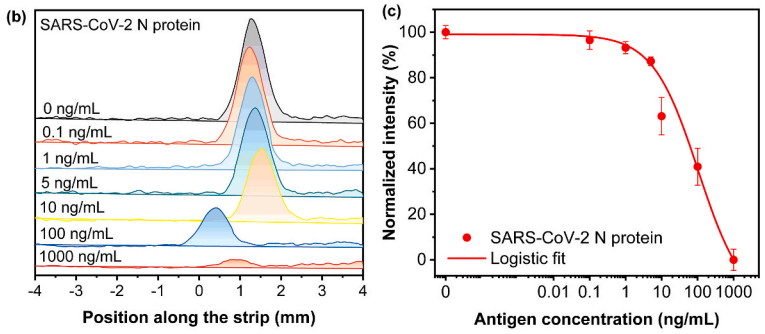

Fig. 4. Illustration of competitive SELFIA assays with FND reporter (a). In competitive SELFIA, samples were first incubated with antibody-conjugated FND before being dropped onto the antigen-immobilized test trip. When the sample contains the target antigen (positive), the antigen will form immunocomplex with antibodies on the FND surface. The FND particles will not be captured by the antigen immobilized on the test strip. When the sample does not contain the target antigen (negative), the antibody-conjugated FND will be captured by the antigen immobilized on the test strip, generating a strong fluorescent signal. Competitive SELFIA assays (b) and normalized fluorescent intensity (c) for SARS-CoV-2 nucleocapsid antigen using anti-chicken IgG antibody-conjugated FND. The solid curve is the best fit of the experimental data to a logistic function, $y = a_2 + (a_1 + a_2)/(1 + (x/x_0)^p)$, where a_1, a_2, x_0, and p are constants. (n = 3).

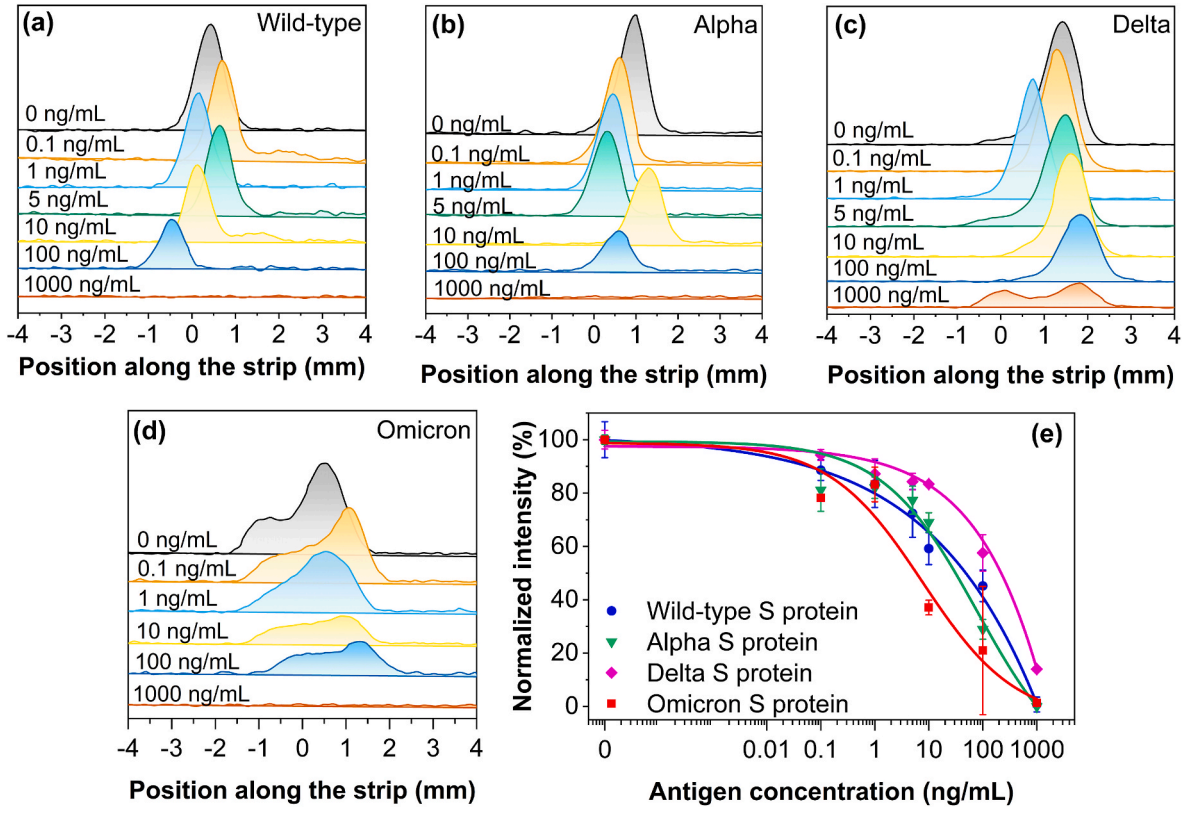

Fig. 5. Competitive SELFIA assays for SARS-CoV-2 spike antigen from (a) wild-type, (b) Alpha, (c) Delta, and (d) Omicron variants using S44F antibody-conjugated FND. (e) Normalized fluorescent intensity of competitive SELFIA for SARS-CoV-2 S antigen detection. The solid curve is the best fit of the experimental data to a logistic function, $y = a_2 + (a_1 + a_2)/(1 + (x/x_0)^p)$, where a_1, a_2, x_0, and p are constants.

complicated, and the complex nature of the biological sample may interfere with the test result since it relies on the distance between Gd and ND. In comparison, our SELFIA platform is based on the magnetic modulation of FND to obtain background-free detection. The magnetic field ($f = 102.4$ Hz, $B = 40$ mT) was optimized for FND and is demonstrated to have no interference with the biological sample [28]. In addition, the SELFIA assay is simple, cost-effective, and rapid compared with other commonly used tests such as RT-PCR and ELISA. As shown in Table S2, an ELISA assay could take up to 2–5 h to process and requires complex sample preparation, laboratory equipment, and professional training. In contrast, with buffering and assay optimization, the SELFIA can be comparable to ELISA in terms of sensitivity and specificity with the advantages of a rapid test (simple, low-cost).

4. Conclusion

We proposed the SELFIA platform based on the magnetic modulation of NV^- centers in FND for the detection of SARS-CoV-2 N and S antigens. The SELFIA assay indicated that the anti-S S44F antibody could efficiently detect S antigens from various SARS-CoV-2 variants (wild-type, Alpha, Delta, and Omicron). Competitive SELFIA assay enhanced the sensitivity up to 50-fold with a LOD of 0.77–1.94 ng/mL (4.4–11.0 pM) compared to the direct format. The present SELFIA platform is simple, rapid, cost-effective, and scalable. As we have seen, whereas a direct SELFIA assay could be used for antibody/antigen pair screening in diagnosis development, the competitive SELFIA assay could be mobilized as an accurate quantitative diagnostic tool. In addition to having significant implications for the control of the COVID-19 pandemic, these findings could also help mitigate future disease outbreaks, more generally.

CRediT authorship contribution statement

Wesley Wei-Wen Hsiao: Conceptualization, Methodology, Writing – original draft, Writing – review & editing, Supervision, Funding acquisition. **Neha Sharma:** Investigation, Data curation, Writing – original draft, Visualization. **Trong-Nghia Le:** Methodology, Validation, Formal analysis, Writing – original draft, Writing – review & editing, Visualization. **Yu-Yuan Cheng:** Investigation. **Cheng-Chung Lee:** Methodology, Resources. **Duc-Thang Vo:** Writing – original draft, Writing – review & editing. **Yuen Yung Hui:** Methodology, Writing – review & editing. **Huan-Cheng Chang:** Conceptualization, Methodology, Supervision, Writing – review & editing. **Wei-Hung Chiang:** Conceptualization, Methodology, Supervision, Writing – review & editing, Funding acquisition.

Declaration of competing interest

The authors declare that they have no known conflict interests or personal relationships that could have appeared to influence the work reported in this paper.

Data availability

Data will be made available on request.

Acknowledgments

This research was funded by the projects of the Taiwan Ministry of Science and Technology (MOST): MOST 110-2222-E-011-004, 110-2628-E-011 -003, 109-2923-E-011 -003 -MY3, & 111-NU-E-011-001-NU.

Appendix A. Supplementary data

Supplementary data to this article can be found online at https://doi.org/10.1016/j.aca.2022.340389.

References

[1] M. Ciotti, M. Ciccozzi, A. Terrinoni, W.C. Jiang, C.B. Wang, S. Bernardini, The COVID-19 pandemic, Crit. Rev. Clin. Lab Sci. 57 (2020) 365–388.
[2] K. Yuki, M. Fujiogi, S. Koutsogiannaki, COVID-19 pathophysiology: a review, Clin. Immunol. 215 (2020), 108427.
[3] K. Leung, M.H. Shum, G.M. Leung, T.T. Lam, J.T. Wu, Early transmissibility assessment of the N501Y mutant strains of SARS-CoV-2 in the United Kingdom, October to November 2020, Euro Surveill. 26 (2021).
[4] A.J. Greaney, A.N. Loes, K.H.D. Crawford, T.N. Starr, K.D. Malone, H.Y. Chu, J. D. Bloom, Comprehensive mapping of mutations in the SARS-CoV-2 receptor-binding domain that affect recognition by polyclonal human plasma antibodies, Cell Host Microbe 29 (2021) 463–476, e466.
[5] D.W. Eyre, D. Taylor, M. Purver, D. Chapman, T. Fowler, K.B. Pouwels, A. S. Walker, T.E.A. Peto, Effect of covid-19 vaccination on transmission of Alpha and Delta variants, N. Engl. J. Med. 386 (2022) 744–756.
[6] Y. Araf, F. Akter, Y.-d. Tang, R. Fatemi, M.S.A. Parvez, C. Zheng, M.G. Hossain, Omicron variant of SARS-CoV-2: genomics, transmissibility, and responses to current COVID-19 vaccines, J. Med. Virol. 94 (2022) 1825–1832.
[7] B. Giri, S. Pandey, R. Shrestha, K. Pokharel, F.S. Ligler, B.B. Neupane, Review of analytical performance of COVID-19 detection methods, Anal. Bioanal. Chem. 413 (2021) 35–48.
[8] R. Jalandra, A.K. Yadav, D. Verma, N. Dalal, M. Sharma, R. Singh, A. Kumar, P. R. Solanki, Strategies and perspectives to develop SARS-CoV-2 detection methods and diagnostics, Biomed. Pharmacother. 129 (2020), 110446.
[9] W. Wang, Y. Xu, R. Gao, R. Lu, K. Han, G. Wu, W. Tan, Detection of SARS-CoV-2 in different types of clinical specimens, JAMA 323 (2020) 1843–1844.
[10] L. Yu, S. Wu, X. Hao, X. Dong, L. Mao, V. Pelechano, W.H. Chen, X. Yin, Rapid detection of COVID-19 coronavirus using a Reverse transcriptional loop-mediated isothermal amplification (RT-LAMP) diagnostic platform, Clin. Chem. 66 (2020) 975–977.
[11] W.W. Hsiao, T.N. Le, D.M. Pham, H.H. Ko, H.C. Chang, C.C. Lee, N. Sharma, C. K. Lee, W.H. Chiang, Recent advances in novel lateral flow technologies for detection of COVID-19, Biosensors 11 (2021).
[12] W. Zeng, G. Liu, H. Ma, D. Zhao, Y. Yang, M. Liu, A. Mohammed, C. Zhao, Y. Yang, J. Xie, C. Ding, X. Ma, J. Weng, Y. Gao, H. He, T. Jin, Biochemical characterization of SARS-CoV-2 nucleocapsid protein, Biochem. Biophys. Res. Commun. 527 (2020) 618–623.
[13] H. Xi, H. Jiang, M. Juhas, Y. Zhang, Multiplex biosensing for simultaneous detection of mutations in SARS-CoV-2, ACS Omega 6 (2021) 25846–25859.
[14] C. Dobaño, R. Santano, A. Jiménez, M. Vidal, J. Chi, N. Rodrigo Melero, M. Popovic, R. López-Aladid, L. Fernández-Barat, M. Tortajada, F. Carmona-Torre, G. Reina, A. Torres, A. Mayor, C. Carolis, A.L. García-Basteiro, R. Aguilar, G. Moncunill, L. Izquierdo, Immunogenicity and crossreactivity of antibodies to the nucleocapsid protein of SARS-CoV-2: utility and limitations in seroprevalence and immunity studies, Transl. Res. 232 (2021) 60–74.
[15] A. Mittal, K. Manjunath, R.K. Ranjan, S. Kaushik, S. Kumar, V. Verma, COVID-19 pandemic: insights into structure, function, and hACE2 receptor recognition by SARS-CoV-2, PLoS Pathog. 16 (2020), e1008762.
[16] F. Amanat, D. Stadlbauer, S. Strohmeier, T.H.O. Nguyen, V. Chromikova, M. McMahon, K. Jiang, G.A. Arunkumar, D. Jurczyszak, J. Polanco, M. Bermudez-Gonzalez, G. Kleiner, T. Aydillo, L. Miorin, D.S. Fierer, L.A. Lugo, E.M. Kojic, J. Stoever, S.T.H. Liu, C. Cunningham-Rundles, P.L. Felgner, T. Moran, A. Garcia-Sastre, D. Caplivski, A.C. Cheng, K. Kedzierska, O. Vapalahti, J.M. Hepojoki, V. Simon, F. Krammer, A serological assay to detect SARS-CoV-2 seroconversion in humans, Nat. Med. 26 (2020) 1033–1036.
[17] C.A. Ascoli, Could mutations of SARS-CoV-2 suppress diagnostic detection? Nat. Biotechnol. 39 (2021) 274–275.
[18] G. Lippi, K. Adeli, M. Plebani, Commercial immunoassays for detection of anti-SARS-CoV-2 spike and RBD antibodies: urgent call for validation against new and highly mutated variants, Clin. Chem. Lab. Med. 60 (2022) 338–342.
[19] D.K. Agarwal, V. Nandwana, S.E. Henrich, V.P.V.N. Josyula, C.S. Thaxton, C. Qi, L. M. Simons, J.F. Hultquist, E.A. Ozer, G.S. Shekhawat, V.P. Dravid, Highly sensitive and ultra-rapid antigen-based detection of SARS-CoV-2 using nanomechanical sensor platform, Biosens. Bioelectron. 195 (2022), 113647.
[20] J.-H. Lee, Y. Lee, S.K. Lee, J. Kim, C.-S. Lee, N.H. Kim, H.G. Kim, Versatile role of ACE2-based biosensors for detection of SARS-CoV-2 variants and neutralizing antibodies, Biosens. Bioelectron. 203 (2022), 114034.
[21] C. Zhang, T. Zheng, H. Wang, W. Chen, X. Huang, J. Liang, L. Qiu, D. Han, W. Tan, Rapid one-pot detection of SARS-CoV-2 based on a lateral flow assay in clinical samples, Anal. Chem. 93 (2021) 3325–3330.
[22] B.-M. Chang, H.-H. Lin, L.-J. Su, W.-D. Lin, R.-J. Lin, Y.-K. Tzeng, R.T. Lee, Y.C. Lee, A.L. Yu, H.-C. Chang, Highly fluorescent nanodiamonds protein-functionalized for cell labeling and targeting, Adv. Funct. Mater. 23 (2013) 5737–5745.
[23] L.P. Suarez-Kelly, S.H. Sun, C. Ren, I.V. Rampersaud, D. Albertson, M.C. Duggan, T. C. Noel, N. Courtney, N.J. Buteyn, C. Moritz, L. Yu, V.O. Yildiz, J.P. Butchar, S. Tridandapani, A.A. Rampersaud, W.E. Carson 3rd, Antibody conjugation of fluorescent nanodiamonds for targeted innate immune cell activation, ACS Appl. Nano Mater. 4 (2021) 3122–3139.
[24] T.A. Dolenko, S.A. Burikov, K.A. Laptinskiy, T.V. Laptinskaya, J.M. Rosenholm, A. A. Shiryaev, A.R. Sabirov, I.I. Vlasov, Study of adsorption properties of functionalized nanodiamonds in aqueous solutions of metal salts using optical spectroscopy, J. Alloys Compd. 586 (2014) S436–S439.
[25] A. Krueger, D. Lang, Functionality is key: recent progress in the surface modification of nanodiamond, Adv. Funct. Mater. 22 (2012) 890–906.

[26] L.J. Su, M.S. Wu, Y.Y. Hui, B.M. Chang, L. Pan, P.C. Hsu, Y.T. Chen, H.N. Ho, Y. H. Huang, T.Y. Ling, H.H. Hsu, H.C. Chang, Fluorescent nanodiamonds enable quantitative tracking of human mesenchymal stem cells in miniature pigs, Sci. Rep. 7 (2017), 45607.
[27] Y.R. Chang, H.Y. Lee, K. Chen, C.C. Chang, D.S. Tsai, C.C. Fu, T.S. Lim, Y.K. Tzeng, C.Y. Fang, C.C. Han, H.C. Chang, W. Fann, Mass production and dynamic imaging of fluorescent nanodiamonds, Nat. Nanotechnol. 3 (2008) 284–288.
[28] Y.Y. Hui, O.J. Chen, H.H. Lin, Y.K. Su, K.Y. Chen, C.Y. Wang, W.W. Hsiao, H. C. Chang, Magnetically modulated fluorescence of nitrogen-vacancy centers in nanodiamonds for ultrasensitive biomedical analysis, Anal. Chem. 93 (2021) 7140–7147.
[29] B.D. Grant, C.E. Anderson, J.R. Williford, L.F. Alonzo, V.A. Glukhova, D.S. Boyle, B. H. Weigl, K.P. Nichols, SARS-CoV-2 coronavirus nucleocapsid antigen-detecting half-strip lateral flow assay toward the development of point of care tests using commercially available reagents, Anal. Chem. 92 (2020) 11305–11309.
[30] S. Hosseini, P. Vázquez-Villegas, M. Rito-Palomares, S.O. Martinez-Chapa, Advantages, disadvantages and modifications of conventional ELISA, in: S. Hosseini, P. Vázquez-Villegas, M. Rito-Palomares, S.O. Martinez-Chapa (Eds.), Enzyme-linked Immunosorbent Assay (ELISA): from A to Z, Springer Singapore, Singapore, 2018, pp. 67–115.
[31] S. Sakamoto, W. Putalun, S. Vimolmangkang, W. Phoolcharoen, Y. Shoyama, H. Tanaka, S. Morimoto, Enzyme-linked immunosorbent assay for the quantitative/qualitative analysis of plant secondary metabolites, J. Nat. Med. 72 (2018) 32–42.
[32] J.H. Bong, T.H. Kim, J. Jung, S.J. Lee, J.S. Sung, C.K. Lee, M.J. Kang, H.O. Kim, J. C. Pyun, Competitive immunoassay of SARS-CoV-2 using pig sera-derived anti-SARS-CoV-2 antibodies, Biochip J. 15 (2021) 100–108.
[33] C. Li, R. Soleyman, M. Kohandel, P. Cappellaro, SARS-CoV-2 quantum sensor based on nitrogen-vacancy centers in diamond, Nano Lett. 22 (2022) 43–49.